Experimental Setup for Field Oriented Control of AC Induction Motors

Benjamin Kuchen
Instituto de Automática
Universidad Nacional de San Juan
Av. Lib. San Martín 1109 (0)
5400 San Juan
ARGENTINA

Manuel Armada, Carlos Vargas
Instituto de Automática Industrial, CSIC

C.N. III, Km 22,800 La Poveda
28500 Arganda del Rey, Madrid
SPAIN

Daniel Carrica
Universidad Nacional de Mar del Plata
Lab. de Instrum. y Control
ARGENTINA

Abstract: An experimental system for controlling AC induction motors using Field Oriented Control (FOC) strategies is presented. FOC Theory requires control loops for statoric currents and Pulse Width Modulation (PWM) techniques for controlling the power inverter. This work covers both items and summarizes the fundamentals of FOC theory. The general architecture of the system and the IGBT power inverter are also described.

1. Introduction

Since Hasse [3] proposed FOC in 1969, a theory later formalized by Blaschke [1] in 1973, this method has been replacing all previous kind of induction motor control as a result of its improved dynamic characteristics. Field Oriented Control (FOC) is primarily based on establishing a coordinate system for representing the AC motor currents and voltages, which takes as reference the rotoric magnetic field, thereby allowing independent control for the rotoric magnetic current (field control) and for the torque current. This way, AC induction motor control becomes similar to DC motor control, where the field and armature or torque currents are naturally uncoupled and can be independently controlled.
Though AC induction motor control with FOC is obviously more complex than DC motor control, the unquestionable fact that AC motors are ubiquitous, unexpensive and sturdily built machines, along with the possibility of obtaining equivalent dynamic characteristics for both motor types, FOC turns AC motors competitive for use in motion control in mid and high power ratings.

2. Fundamentals of FOC Theory

Several authors [4][5][8] have broadly dealt with FOC fundamentals, which will be briefly described hereon. The mathematical model in a vectorial notation for an AC induction motor is shown in Eqs. 1 to 4.

$$R_S \mathbf{i}_S(t) + L_S \frac{d\,\mathbf{i}_S(t)}{dt} + L_m \frac{d}{dt}(\mathbf{i}_R e^{j\varepsilon}) = \mathbf{u}_S(t) \quad (1)$$

$$R_R \mathbf{i}_R(t) + L_R \frac{d\,\mathbf{i}_R(t)}{dt} + L_m \frac{d}{dt}(\mathbf{i}_S e^{-j\varepsilon}) = 0 \quad (2)$$

$$J\frac{d\omega}{dt} = \frac{2}{3}\mathrm{Im}[\mathbf{i}_S \mathbf{i}_R(t)^* e^{j\varepsilon}] - m_L = m_M - m_L \quad (3)$$

$$\frac{d\,\varepsilon}{d\,t} = \omega \quad (4)$$

where $\mathbf{i}_S$, $\mathbf{i}_R$ are the statoric and rotoric current vectors, respectively, and v_S is the statoric voltage vector. L_S, L_R and L_m are the statoric, rotoric and mutual inductances and R_S, R_R the statoric and rotoric resistances, ε is the angle formed by the rotor's reference position and the stator reference axis, m_M and m_L are the motor and load torques, respectively. J is the moment of inertia of the motor under load and ω is the angular velocity of the motor shaft. Eqs. 1 to 4 are vector differential equations valid for any voltage and current waveform, under variable load and speed.

$$\mathbf{i}_{mR} = \frac{\Phi}{Lm} = \mathbf{i}_S + (1+\sigma_R)\mathbf{i}_R e^{j\varepsilon} = i_{mR} e^{j\rho(t)} \quad (5)$$

FOC is essentially based on the attainment of a reference system which rotates referred to the stator. The electrical magnitudes in this system keep relation to the amplitude of the corresponding stator-referred alternate signals; that is, they are DC-type signals which tend to constant values under steady state

conditions. An appropriate reference system for FOC is the one defined by the rotoric flux represented, in turn, by the rotoric magnetization current i_{mR}, shown in Eq. 5. There, σ_R is the rotoric magnetic leakage factor.

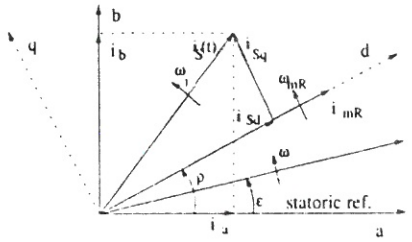

Figure 1 Field Coordinate System

Figure 1 depicts this d-q reference system, in alignment with the rotoric magnetization current, which rotates with an angle $\rho(t)$ respecting the a-b stator-fixed coordinate system. The statoric current and voltage vectors can be projected on the d-q axes, thus

$$i_S e^{-j\rho} = i_{Sd} + j\, i_{Sq} \qquad (6)$$

$$u_S e^{-j\rho} = u_{Sd} + j\, u_{Sq} \qquad (7)$$

$$T_R \frac{d i_{mR}}{dt} + i_{mR} = i_{Sd} \qquad (8)$$

$$\frac{d\rho}{dt} = \omega_{mR} = \omega + \frac{i_{Sq}}{T_R i_{mR}} \qquad (9)$$

resulting, Eqs. 5 to 7 can be replaced by Eqs. 1 to 3 of the AC induction motor model, thus obtaining the same model but represented in field coordinates. This model is free from rotoric currents, a very useful fact, because they cannot be measured in a squirrel-cage motor. From the above replacements, the following equations result.

$$m_M = \frac{2}{3} \cdot \frac{L_m}{1+\delta_R} i_{mR} i_{Sq} \qquad (10)$$

$$m_M = K i_{mR} i_{Sq}$$

Eq.10 shows that the motor torque, expressed in the rotoric field reference system, is proportional to the i_{mR} i_{Sq} product. This means that the torque caused by the AC induction motor can be independently controlled by the rotoric current or the magnetizing current. This feature is of great importance and actually represents the FOC's key factor for governing an AC machine with good dynamic characteristics. Eq.10 closely resembles the one representing the DC motor torque, which is proportional to the field current times armature current product. In like manner, it is possible to attain a speed control by using the excitation current (field control) at above-nominal angular speeds, or by using the torque current (armature control) at lower-than-nominal angular speeds.

The magnitude for i_{mR} must be determined by i_{Sd}, a condition involving a dynamic relationship derived, in turn, by the time constant T_R as expressed by Eq.8. In the control range from zero up to nominal speed, the excitation current is kept constant and the control variable will be the quadrature component i_{Sq}, namely the torque current. This current component is proportional to the motor torque and consequently, allows for obtaining fast dynamic responses.

This control method requires that the angular position for the rotoric flux vector (angle ρ) be known at any one moment. Since its direct measurement with Hall-effect sensors or sensing coils is rather cumbersome, it is preferable to attain this angle by computations on the field-coordinate flux model as represented by Eqs.8 and 9. The inputs for this models are the statoric current i_s and the motor angular speed ω, both magnitudes measurable with standard instruments. The model's outputs are i_{mR} and, by integrating Eq.9, angle ρ. The precision of the results will depend on the value of T_R, which depends, in turn, on the temperature. In the literature [5], various methods for on-line estimating T_R are described.

Figure 2 shows the block diagram for a FOC. The inverter is assumed to act as a controlled current amplifier capable of faithfully following the three-phase reference currents $i_{s1r}, i_{s2r}, i_{s3r}$ which stem from the transformation of the two-phase system i_{ar}, i_{br}. These

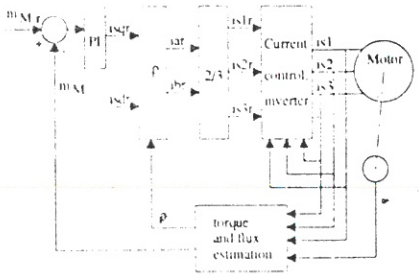

Figure 2 - FOC General Scheme

currents, which are alternate-type in statoric coordinates, are obtained by transforming the direct-type currents i_{Sdr}, i_{Sqr} into field coordinates and based on the instantaneous value of ρ. The remaining parts of the control system are conventional in nature and equivalent to a DC motor control loop. Thus, it is possible to control

the magnetization current (decreasing the flux) by means of the current reference i_{Sdr} or the torque current by means of its reference i_{Sqr}.

The developed motor torque m_M can be computed with Eq.10 and, therefore controlled (acceleration control) by comparing it with a reference torque m_{Mr} as given by a speed control loop. Likewise, it is possible to add a conventional position control loop.

3. Control of Statoric Currents

In FOC applications, the voltage-fed inverters dominate over the current-fed inverters due to their better dynamic performance and smaller torque fluctuation. As they are intrinsically voltage sources, these inverters must be implemented as controlled curren sources with very fast dynamic response in order to satisfy the bandwidth requirements posed by FOC. Therefore, a control loop should be added which, by comparing the measured currents with the reference currents, could govern the inverter with a PWM-type modulation. Figure 3 presents the general scheme for a voltage-fed and current-controlled inverter (VSCI).

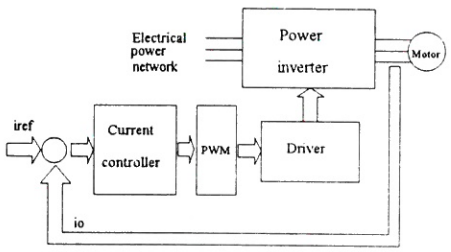

Figure 3 - Voltage-supplied and Current-Controlled Inverter

The main choices for determining the switching sequence for the inverter's electronic switches are

a) ON-OFF loop with hysteresis [5].
b) PWM modulation by carrier wave [5]
c) Patterns with predefined harmonic contents [2]
d) Switching based on the voltage state vector [6,8]

Choice a) leads to a simple hardware implementation based on comparing both measured and reference currents, by using individual comparators and ON-OFF controllers with hysteresis. Its drawbacks will be a high switching frequency, a high ripple and a lack of control on the current waveform harmonics.

Choice b) involves the comparison of a reference waveform having an instantaneous frequency f_m with a triangular waveform of fixed-amplitude and frequency f_p. This latter frequency determines the switching frequency of the inverter electronic switches. For high statoric frequencies, it is suggested to synchronize both waveforms, f_p being an odd multiple of three respecting f_m. Its disadvantage lies on the relatively large harmonics generated at frequencies $f_p = \pm 2 f_m$. The highest modulation index attainable is 78.5%. To take further advantage of the inverter supply, it is possible to overmodulate at the cost of increasing the harmonics content, or else, to add multiple-of-three harmonic components to the reference waveform in order to increase the modulation index.

From the viewpoint of harmonic components of the resulting waveform, choice c) is optimal. As from fixing a number **M** of commutations per quarter of a period, a solution involving Fourier series and **M** coefficient equations can be set forth [2]. The numerical solution for this system of transcendental-type non-linear equations allows for computing the commutation instants which synthesize a PWM waveform. Up to **M-1** harmonics can be eliminated from this waveform. This choice also enables a reduced level of inverter switching frequency with a waveform having a smaller harmonic content and a maximun modulation index close to one. The great complexity in computing prevents from reaching a solution and an implementation in real time. It is preferred therefore, to store in advance the off-line precomputed tables for later use in real time.

Choice d) leads to a very good solution with respect to the number of commutations per period. It is based on finding an optimal sequence for the eight possible inverter switching states which give rise to the various instantaneous voltages set on the statoric coils [6][8]. Several authors [7][9] have proposed other solutions for generating a statoric current vector whose arrowhead describes a circle, closest to perfect as possible (sinusoidal projection). With this option, it is also possible to evaluate the state sequence in real time, thus making this one an interesting alternative to implementation.

4. VSCI Topology and Technology

The circuit topology of a three-phase VSCI is shown in Figure 4. The technology used for the VSCI electronic switches is IGBT-type (Insulated Gate Bipolar Transistor). This technology has the same advantages as those found in MOSFETs, specially at the switches' inputs, with very low driving power requirements. Though IGBTs are slower than MOSFETs, they are better as regards the power ratings they can control, the voltage levels they can withstand, and due to their smaller conduction losses. Their slower response does not pose serious limitations, for these devices can handle switching frequencies of up to 15 Khz, with standard IGBT technology, and up to 50 Khz, with ultrafast IGBT technology.

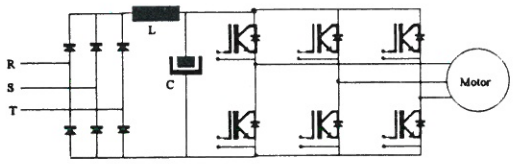

Figure 4 -VSCC Circuit Topology

The driving electronics grows in complexity according to insulation requirements due to high voltages on the "high-side" elements on each circuit branch, and to fast-response protection requirements against overcurrent on the load and undervoltage of the source.

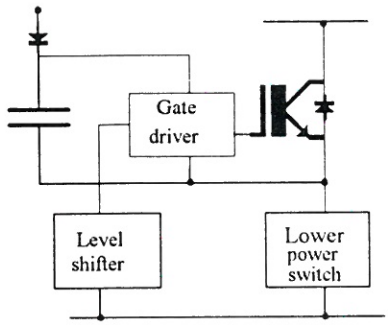

Figure 5 -Bootstrap Capacitor Voltage Source

The first protection uses the so-called bootstrap capacitor insulation as depicted in Figure 5. When the "low-side" electronic switch is turned on, capacitor C charges up to the supply voltage level which feeds the electronic circuitry, thus being capable of later feeding the driver on the "high-side".

5. Experimental Development

For this specific application a three-phase IGBT model is used, with six switches and freewheel diodes as well. The specifications for maximum voltage and maximum current are 1200 V and 30 A, respectively, which enables to handle power ratings of up to 13 Kw. For implementations oriented to AC motor control and regarding a 0.9 power factor, an AC motor efficiency of 80%, an extrafundamental harmonic content of 10% and assuming a 180 % overload for the inverter (to account for motor startup, etc.), three-phase motors of up to 5 Kw can be operated with this inverter.

The driving electronics was implemented around the IC IR2130 which makes use of the bootstrap capacitor technique. Such a circuit can drive a complete three-phase inverter fed with supply voltages of up to 600 V. This device internally impedes any occasional turn-on of both switches on a branch, thus preventing a shortcircuit condition. It also inserts time delays between ON-OFF positions of consecutive switches on a branch, that is, a time delay is set between switch 1 turn-off and switch 2 turn-on. The circuit is protected against load overcurrents and source undervoltages or low voltages on each "high-side" drivers. In the presence of any such condition, every IGBT gets deactivated. The drivers can generate currents ranging from +250 mA to -500 mA, thus resulting switching times of 75/35 ns for IGBTs having input capacitance of about 1000 pF.

As to inverter operation, and considering the experimental characteristic of the present work, a structure based on real-time scanning of a precomputed table was adopted. This precomputed table scanning allows for using switching patterns of any alternative stated in **3**, enabling the contrast of results as well.

The table scanning speed defines the frequency for the fundamental harmonics of the switching pattern which controls the inverter, while there exists a specific pattern for each modulation index. With an adequate selection of the patterns in terms of the frequency to be generated, it is possible to keep the inverter switching frequency approximately constant.

For current open-loop applications, to handle the switching pattern table simply means associating a definite pattern with each switching frequency, which allows for keeping V/f constant, that is, constant flux. For closed-loop applications, the frequency channel, or table scanning speed, must be controlled independently of the magnitude channel, which is the channel that selects a predetermined pattern. The table handling must be performed so as to allow for both frequency and magnitude being instantaneously changed without giving rise to significant transients. The number of patterns (magnitudes) was fixed in 2^7, whilst the angular resolution was fixed in 2^{10} per quarter of cycle in order to satisfy the various switching conditions with acceptable precision.

The control system with current-controlled inverter was implemented, in its experimental stage, on a 80486 50 MHz computer, having an input-output board with the necessary elements for carrying out the control in real time, such as A/D, D/A converters, programmable timers and interruption handling. In a first stage, the precomputed switching patterns based on the modulation by triangular carrier-wave were used, also foreseeing the experimentation with patterns optimized as to harmonic content. The current loop was sampled with a period of 500 ms and in the amplitude channel a simple integrative proportional controller was used.

The inverter is fed by means of a complete-waveform three-phase rectifier and an LC filter which ensures a

540 V supply voltage. The inverter feeds a 1 Kw six-pole squirrel-cage motor which a tacheometer and a 500-line incremental encoder were added to.

6. Results

The experimental system was tested as a whole assembly, special attention being paid to the behaviour of the statoric current control loop due to its critical importance. The proposed electronic solution was validated, as regards power and control aspects. The vector control (FOC) algorithms were tested at simulation level though not included in the torque control loop. No serious difficulties are anticipated for reaching sampling times of less-than-one millisecond in computing the complete control algorithm.

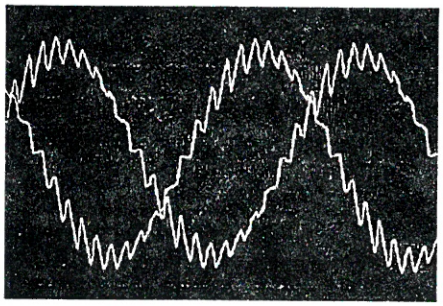

Figure 6 -Statoric Currents (f_p/f_m = 21)

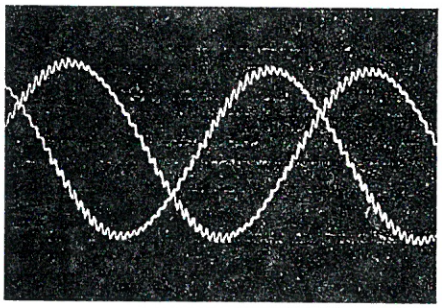

Figure 7 -Statoric Currents (f_p/f_m=45)

Several tests were carried out for determining the best characteristics of PWM patterns and the most appropriate switching frequencies. At low frequency range, patterns with up to 345 commutations per cycle with an angular discrimination of 4,096 points, were performed.

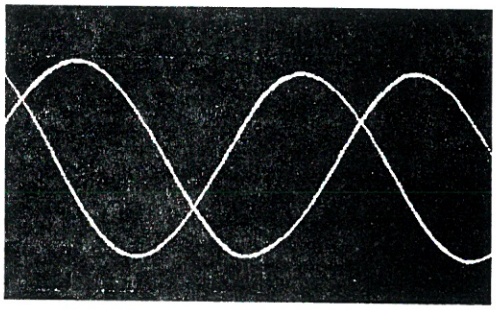

Figure 8 -Statoric Currents (f_p/f_m=153)

Figures 6, 7 and 8 show the statoric currents i_{s_1}, i_{s_2} measured with Hall-effect sensors for various f_p / f_m values. From there, the excellent waveforms obtained and the presence of a larger ripple content for lower f_p / f_m values are apparent. The AC motor was tested under variable load conditions and with fixed references for statoric currents, thus attaining a fast dynamic response for the primary current loop. The operation of this control loop implies a correct processing of the precomputed pattern tables for the various modulation indexes and switching frequencies.

7. Conclusions

When considering the level of circuit integration reached at present and other state-of-the-art electronic technologies, the complete implementation of a vectorial control system for conventional AC squirrel-cage motors appears as a promissory and competitive alternative. Notwithstanding the fact that for this work a not-very-high level of integration was reached, the results obtained were satisfactory as for a technological solution for driving-power and statoric current control, in themselves the most critical aspects of the control system. The experience attained in handling and implementing the switching patterns is regarded as essential for further development. Although the final implementation is based on a DSP-type dedicated microprocessor, the use of a general-purpose computing system has been proven as a good alternative for the experimentation phase.

Acknowledgment

The authors want to acknowledge the support received from the DG XIII of CEC on their project "Advanced Robot Control with Multisensor Integration" (ROCOMI ECLA 02/76100).

REFERENCES

1 BLASCHKE, F., **The Principle of Field Orientation as Applied to the New Transvector Closed Loop System for Rotating Field Machines**, SIEMENS REVIEW, July 1972. pp. 217-223

2 ENJETI, P. et al, **A New PWM Speed Control System for High-Performance AC Motor Drives**, IEEE TR. ON INDUSTRIAL ELECTRONICS, vol.37, No.2, 1990, pp. 143-151.

3 HASSE, K., **Zur Dynamik drezahlgeregelter Antriebe mit stromrichteergespeisten Asynchron-Kurzschlusslaüfermotoren**, Diss. TH, Darmstadt, FRG, 1969.

4 HOLZ, J., **Field-Oriented Asynchronous Pulse-Width Modulation for High-Performance AC Machine Drives Operating at Low Switching Frequency**, IEEE TR. ON INDUSTRY APPLICATIONS, vol.27, no.3, 1991, pp.574-581.

5 LEONHARD, W., **Control of Electrical Drives**. Ch.10-12, SPRINGER-VERLAG Berlin,, 1990.

6 MIKI, I. et al., **A New Simplified Current Control Method for Field-Oriented Induction Motor Drives**, IEEE TR. ON INDUSTRY APPLICATIONS, Vol.27,no.6,1991, pp.1081-1086.

7 MURAI,Y., **High-Frequency Split Zero-Vector PWM with Harmonics Reduction for Induction Motor Drives**, IEEE TR. ON INDUSTRY APPLICATIONS, Vol.28, No.1, 1992, pp. 105-112.

8 POLLMANN, A., **Software Pulsewidth Modulation for Microprocessor Control of AC Drives**, IEEE TR. ON INDUSTRY APPLICATIONS, vol. IA-22, no.4, 1986 pp. 691-696.

9 VAN DER BROECK, H., **Analysis and Realization of a Pulsewidth Modulator Based on Voltage Space Vectors**, IEEE TR. ON INDUSTRY APPLICATIONS, Vol. IA-22, No.1, pp. 142-150.